Hoar and D. J. Randall, Eds. (Academic Press, New York, 1971), vol. 5, p. 493; T. Szabo and A. Fessard, in (*8*), p. 59.
8. A. Fessard, Ed., *Handbook of Sensory Physiology*, vol. 3, part 3, *Electroreceptors and Other Specialized Receptors in Lower Vertebrates* (Springer, Berlin, 1974).
9. C. C. Bell and C. J. Russell, *Brain Res.* **145**, 85 (1978).
10. A. J. Kalmijn, in (*8*), p. 147.
11. C. C. Bell and C. J. Russell, *Soc. Neurosci. Abstr.* **2**, 177 (1976).
12. G. N. Andrianov and O. B. Ilynsky, *J. Comp. Physiol.* **86**, 365 (1973); D. B. McCreery, *ibid.* **113**, 317 (1977).
13. T. Szabo, in (*8*), p. 13; R. B. Szamier and M. V. L. Bennett, *J. Morphol.* **143**, 365 (1974).
14. Supported by NSF grant BNS 79-050-96.

17 March 1981; revised 6 June 1981

A New Laser Scanning System for Measuring Action Potential Propagation in the Heart

Abstract. *A rapid laser scanning system was developed to map the spread of excitation in amphibian and mammalian hearts stained with fluorescent dye. Isochronic maps of conduction were constructed by timing the upstroke of the optical action potential; 128 sites could be scanned in 4 milliseconds. The accuracy of this technique was verified by recording simultaneously from 16 unipolar electrodes placed in different areas of the heart. Conducted action potentials in normal frog heart propagated at 0.1 meter per second. Propagation of action potentials was also monitored in ischemic cat heart, in which both driven and arrhythmic action potential upstrokes could be tracked. The results suggest that this system is capable of scanning the normal and abnormal spread of electrical activity in the heart.*

Voltage-sensitive fluorescent and absorption dyes are regularly used to measure action potentials in a variety of excitable tissues (*1–7*). Previously we suggested (*8*) that optical scanning of electrical activity in the heart would be possible if the signal-to-noise ratios of the voltage-sensitive dyes were improved and a sufficiently rapid and versatile scanning system were developed. We now describe a new laser scanning system for mapping the spread of electrical activity in the heart. The system is capable of monitoring changes in membrane potential from 128 to 512 locations in 4 to 16 msec. Amphibian atrium and ventricle and mammalian whole ventricles were scanned optically for the action potential upstroke, and activation maps were constructed. Simultaneous measurements from a grid of 16 Ag-AgCl electrodes and suppression of contraction by using Ca antagonist (Diltiazem, Marion Laboratories) or no Ca^{2+} suggest that the laser scanning system measures the propagation of action potential upstrokes rapidly and reliably, with good spatial and temporal resolution.

The heart of a bullfrog (*Rana catesbeiana*) was removed and perfused through the sinus venosus with Ringer solution containing 116 m*M* NaCl, 3 m*M* KCl, 2 m*M* $NaHCO_3$, and 1 m*M* $CaCl_2$. Ringer solution containing 0.1 mg of WW-781 dye (*9*) per milliliter was admitted to the heart and withdrawn after 5 minutes. The change in fluorescence produced by a single action potential was about 10 percent for the wavelengths collected above 645 nm. In some experiments the intact heart was optically scanned. In experiments that required preparation of a ventricular flap, the ventricle was freed of the atria and opened by incisions along both sides. Numerous fibers crisscrossing the inside of the heart were cut to permit spreading of the ventricular flaps. Such a preparation was pinned onto the Sylgard bottom of a black Perspex dish. Protruding through the dish and flush with the exposed Sylgard surface were 16 Ag-AgCl electrodes (diameter, 500 μm), which were used to record unipolar electrograms or to deliver electrical shocks to the heart. The dish was positioned under the photodetector optics, allowing the laser scanning beam to impinge on the tissue at a small angle from the perpendicular. The He-Ne laser beam was focused to a 130-μm spot with an incident intensity of about 7 mW.

The laser (Jodon HN-20) provides a monochromatic beam of 20 mW at a wavelength of 632.8 nm, with < 0.5 percent (root-mean-square) noise from 120 Hz to 100 kHz. The rapid positioning of the laser beam was achieved by a pair of acousto-optical devices (Intra Action Corp.) (*10, 11*). It was possible to point the laser spot randomly at any part of the heart on a 128-point grid within 5 μsec. The fluorescence elicited from dye-stained tissue was collected and focused through a cut-on filter (Schott RG 645) onto a photodiode (UDT Pin-10). The photodiode signal was processed by a high-bandwidth amplifier (settling time, 25 μsec). Each acousto-optic device deflects the laser beam along one of the perpendicular scan axes to an extent determined by the control signals. The control signals are generated by the scan controller interface under the supervision of programs running within the computer. The actual scan is performed by repeatedly cycling through a list of coordinates, pausing at each site to digitize a fluorescence level and store the reading. Each coordinate corresponds to a site

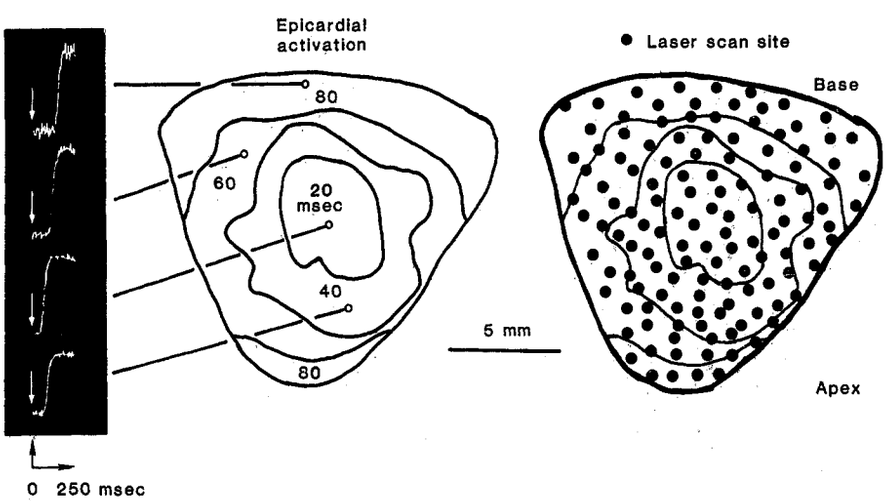

Fig. 1. Epicardial activation in an atrially paced bullfrog ventricle. The map in the center shows contours of activation moments, or isochrones, for action potentials monitored on the epicardial surface of an intact, continuously perfused heart in a Langendorff-type setup. All action potentials occurring 20 msec before the labeled time or sooner are included in a given zone. On the right the same isochrones are shown with dots indicating the 128 sites where action potential upstrokes were recorded and from which the map was constructed. On the left are action potential upstrokes obtained from the sites indicated by open circles and shown as starting at time 0 (white arrows) and continuing for 250 msec. Activation moments were timed as the midpoint of the upstroke of the action potential. Concentration of calcium in the perfusate was 1.0 m*M*; temperature, 20°C.

0036-8075/81/1023-0453$01.00/0

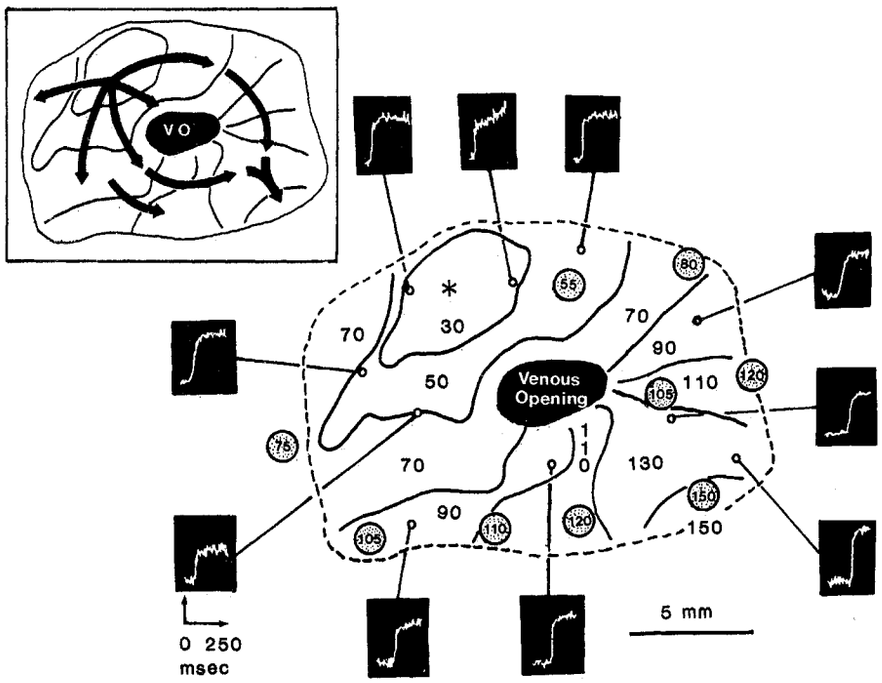

Fig. 2. Electrocardiographic and laser scanning activation maps for a bullfrog atrial sheet. An activation map obtained from a 128-site laser scan and the recordings from a multisite electrogram performed simultaneously show good agreement in this preparation. Twelve of the 16 electrodes were within the scan area. Recordings were taken from nine of them and one was used for stimulation (asterisk). Also shown are action potential upstrokes obtained from the sites indicated by open circles. The inset shows how the activation wave fronts move away from the stimulus site and around the venous opening toward the lower right-hand edge of the tissue.

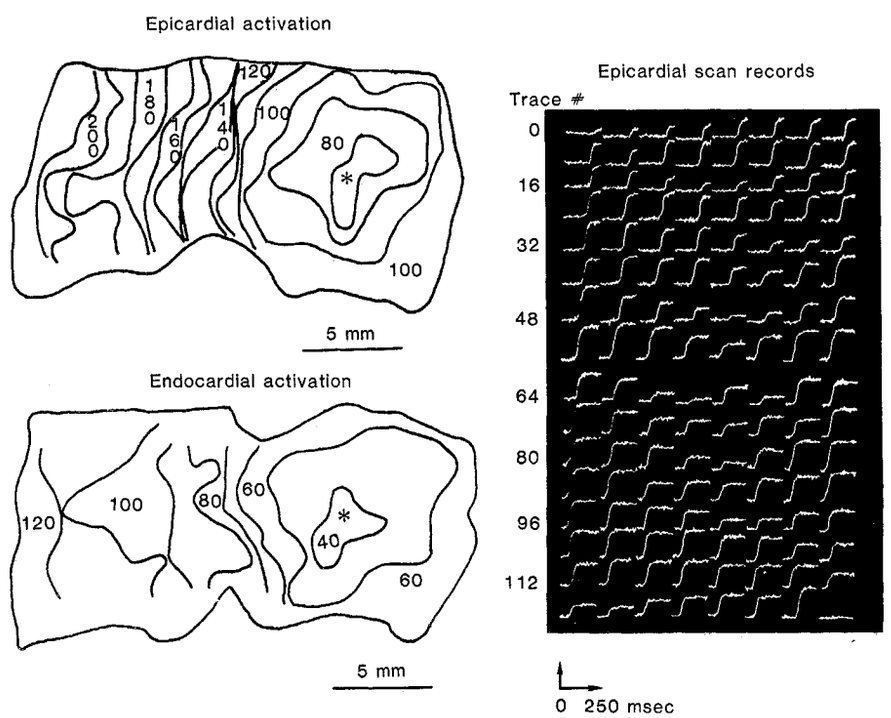

Fig. 3. Epicardial and endocardial activation maps for a bullfrog ventricular flap, showing the spread of activation on both surfaces of the flap. The ventricle was cut along the sides and pinned so that the former apex lay in the middle of the flap while each end corresponded to the base. Isochrones are resolved to 10 msec and every other zone is labeled. The late appearance of activation on the top surface (epicardial scan) is due to the delay in the conduction of the transwall impulse. This delay is eliminated with higher strength shocks, which do not alter the conduction pattern. A complete record of the signals from the epicardial scan is shown on the right. As with the other sample traces, these all start at time 0 and extend for 250 msec. The last record (trace 127), from a nonfluorescent spot, shows the baseline level of noise in the photodetector system. The setting time of the light-measuring system was 25 μsec.

of interest determined before the scan.

To create a list of scan sites, we used a pair of positioning knobs to maneuver the laser beam. If a spot was to be included in the scan pattern, a "put" button was depressed and the spot remained illuminated as the beam was moved elsewhere. As each spot was added to the projected pattern, its coordinates were recorded in a list of points to be scanned. This list was repeatedly examined during the procedure. Each point was sequentially illuminated at high speed, so a continuous projection of the preliminary scan pattern was perceived. A "take" operation was used to remove a spot from consideration.

The scanning operation could be started by a manual trigger, a synchronizing pulse, or a signal from one of the electrogram leads. A selector switch determined whether any scans were to be skipped to allow longer periods of scanning.

Figure 1 shows an activation sequence for the bullfrog ventricular epicardium. Absolute activation moments were measured at the midpoint of the action potential upstroke. The activation times illustrated were calculated relative to the time of the appearance of the first action potential on the surface. All upstrokes occurring within the first 20 msec were drawn within the 20-msec isochrone. Sample action potential upstrokes for various sites are also shown. The signal-to-noise ratio for a particular site was variable and depended on such parameters as the amount of excitable tissue, the degree of staining, and the amount of light collected by the photodetector. The activation map in Fig. 1 shows that excitation in an atrially driven ventricle commences at the center and spreads outward to activate the apex and the base of the epicardial surface. The excitation wave in this preparation was initiated by the normal pacemaker in the atrium, whose impulse is conducted into the ventricle through the atrioventricular ring. Since the depolarization did not proceed in a base-to-apex direction on the epicardium, the results suggest preferential conduction pathways from atrium to ventricle through the underlying endocardium (*12*). This pattern of conduction was preserved if perfusion was stopped and the heart allowed to beat. As the heart became ischemic the conduction wave was significantly retarded, but the propagation pattern remained similar to that observed in normal heart. An epicardial conduction velocity of about 0.1 m/sec was consistently measured in perfused frog heart. This value is in good agreement with conduction

velocities measured previously by conventional techniques (*13*). The electrical propagation wave slowed by one-half in nonperfused ischemic frog hearts.

Figure 2 shows a simultaneous laser scan and multisite electrograms recorded from a thin (transparent) atrial sheet. Electrode activation times correspond fairly closely to the isochrones obtained by detailed (128 points) laser scan. Sample action potential upstrokes from various locations show a somewhat smaller signal-to-noise ratio than those recorded in the ventricle (Fig. 1). The larger ventricular signal may be due to deeper penetration of the laser beam into the ventricular wall. In the atrial preparation the laser beam excites the total thickness of the preparation, giving rise to an action potential signal representative of the total thickness of the tissue. Thus, unlike activation in the ventricle (Fig. 1), activation in the atrium proceeds primarily in two dimensions. This simplified conduction pattern allows independent verification of the accuracy of our technique by a conventional multisite recording method. The impulse starts from the stimulating electrode (Fig. 2, asterisk) and radiates around the venous opening at the center of the atrial sheet, finally merging and invading the lower right corner of the preparation (Fig. 2, inset).

Figure 3 shows a detailed activation map for the endocardial and epicardial surfaces of a ventricular flap preparation. The action potentials were recorded from 128 scan sites on the epicardial surface of the heart. The ventricular flaps were stimulated electrically by an electrode (located at the asterisk). The activation maps show a distinct slowing of the propagation wave (narrowing of isochrones) in the apical region. The laser scan reveals that the endocardial propagation wave spreads nearly twice as fast as it would on the epicardial surface. These results are consistent with epicardial scan patterns for the self-pacing intact heart, in which the signal spreads toward the base and apex of the heart from the midregion of the ventricle (as if the endocardium had been activated before the epicardium; see Fig. 1).

Intact and dissected mammalian hearts were also examined with the laser scanner. Signals from cat, rat, and guinea pig hearts had equal or better quality than those measured in frog heart. The staining procedure was similar to that described for the amphibian hearts. Both the staining and Tyrode's (*14*) solutions were continuously oxygenated. In cat heart, arrhythmia was induced by stopping perfusion for 30 minutes, rendering the tissue ischemic. This produced many arrhythmic events, including echo beats in response to the atrial pacemaker and bouts of ventricular tachycardia. Figure 4 shows the activation of a portion of the cat ventricular epicardial surface in response to apical stimulation and the propagation of the first of a few echo beats that followed. Note that while conduction is slow for the first beat, it is markedly slower for the echo beat. Although we do not know whether reentry or triggered ectopic focus was the cause of the arrhythmia, the slow conduction speed could favor the reentrant phenomenon.

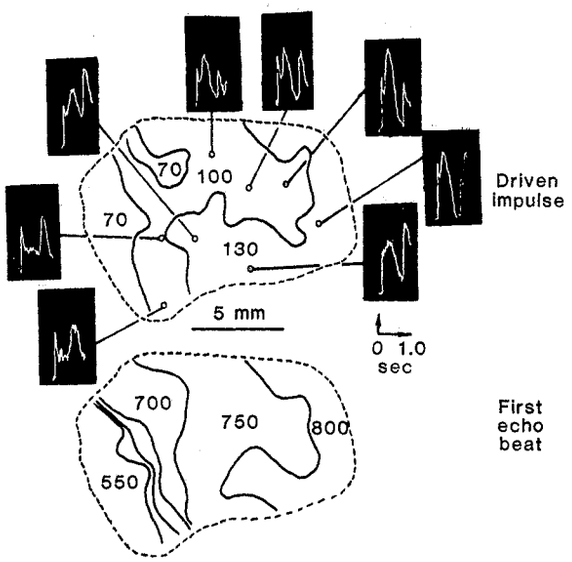

Fig. 4. Epicardial scans of the activation waves in an intact, ischemic cat ventricle. One hundred twenty-eight points on the surface of the heart were scanned. The first driven beat mapped was the result of a stimulus applied to the apex of the heart 80 msec earlier. The first of a series of echo beats is also mapped. The duration of data acquisition was lengthened by skipping scan intervals to decrease the duty cycle. The echo impulse travels somewhat slower and seems to encounter a region with particularly slow conduction on the left. The records show both the driven impulse upstroke and the upstroke of the echo beat, which is easily distinguished from the motion artifact between upstrokes.

Our results suggest that the laser scanner technique can accurately and precisely monitor the spread of electrical activity in the heart. The memory capacity of our system (16 kilobytes) limits our consideration to 128 scan sites for a continuous 252-msec scan. The scan rate (128 sites in 4 msec) is determined by the maximum sensitivity and bandwidth of the photodetector. An improved photodetector system and a powerful computing facility would permit faster scans over much larger areas. The size of the laser scanning beam can be varied by a single optical adjustment; thus one may scan large or small areas with equal facility. We chose a fluorescent dye rather than an absorption dye in order to minimize motion artifact, backscattered laser light, and other nonspecific signals. We were initially concerned with the distortion of the activation signal by the movement of a contracting ventricle. We found that the large signal-to-background ratio for the change in dye fluorescence and the low contrast of the ventricular surface permitted easy discrimination of the abrupt action potential upstrokes from slower movement-related light signals. When gross tissue movement was prohibited it was possible to bathe the tissues in 1.0 to 1.8 m*M* Ca^{2+} solutions without sacrificing scanning accuracy.

We believe that the optical scanning technique can surpass the multielectrode electrographic technique not only by virtue of its greater number of simultaneous measurements, but also by providing the experimenter with a versatile, noninvasive means of directly determining the exact moment of electrical activation of a particular area in the heart. This capability will greatly facilitate the study of impulse propagation in both the normal and diseased heart. The system described in this report should find wide application not only in the study of cellular and organ electrophysiology but in the clinical setting as well.

S. DILLON
M. MORAD

Department of Physiology, University of Pennsylvania, Philadelphia 19104

References and Notes

1. L. B. Cohen and B. M. Salzberg, *Rev. Physiol. Biochem. Pharmacol.* **83**, 35 (1978).
2. B. M. Salzberg, A. Grinvald, L. B. Cohen, H. V. Davila, W. N. Ross, *J. Neurophysiol.* **40**, 1281 (1977).
3. S. M. Baylor, W. K. Chandler, M. W. Marshall, in *Regulation of Muscle Contraction: Excitation-Contraction Coupling*, A. D. Grinnell and M. A. B. Brezier, Eds. (Academic Press, New York, 1981).
4. S. Nakajima and A. Gilai, *J. Gen. Physiol.* **76**, 729 (1980).
5. M. Morad and G. Salama, *J. Physiol. (London)* **292**, 267 (1979).
6. F. Bezanilla and J. Vergara, in *Biophysical Aspects of Cardiac Muscle*, M. Morad, Ed. (Academic Press, New York, 1978).
7. D. M. Senseman and B. M. Salzberg, *Science* **208**, 1269 (1980).
8. G. Salama and M. Morad, *ibid.* **191**, 485 (1976).
9. J. Vergara and F. Bezanilla, *Biophys. J.* **25**, 201 (Abstr.) (1979).
10. The acousto-optic deflector consists of two deflection devices, two voltage-controlled oscillators (50 to 90 MHz), and a series of spherical and

cylindrical lenses. The deflector is composed of a glass substrate with ultrasonic transducers bonded to one end. The oscillator signal is transduced into planar acoustic wave fronts that traverse the length of the glass. The compressions from the peaks and troughs of the waves impose a periodic variation in refractive index throughout the material. In effect, a thick grating with the capability of diffracting visible light is created. A laser beam is introduced, at a small angle, into the aperture and is efficiently diffracted (70 to 90 percent) out at a new angle. The beam steering is accomplished by changing the input oscillator frequency to create a new grating spacing and a different exit angle (*11*).

11. R. Adler, *IEEE Spectrum* **4**, 42 (1967).
12. T. Lewis, *J. Physiol. (London)* **49**, 36 (1915).
13. B. F. Hoffman and P. F. Cranefield, *Electrophysiology of the Heart* (McGraw-Hill, New York, 1960), p. 79.

14. Tyrode's solution (*p*H 7.4) consists of (m*M*) NaCl, 137; KCl, 2.7; $CaCl_2$, 1.8; $MgCl_2$, 0.7; NaH_2PO_4, 0.4; $NaHCO_3$, 12; glucose, 11; and water.

15. We are extremely grateful for the generous gift of WW-781 dye from A. Waggoner.

27 July 1981

Blood-Brain Glucose Transfer: Repression in Chronic Hyperglycemia

Abstract. *Diabetic patients with increased plasma glucose concentrations may develop cerebral symptoms of hypoglycemia when their plasma glucose is rapidly lowered to normal concentrations. The symptoms may indicate insufficient transport of glucose from blood to brain. In rats with chronic hyperglycemia the maximum glucose transport capacity of the blood-brain barrier decreased from 400 to 290 micromoles per 100 grams per minute. When plasma glucose was lowered to normal values, the glucose transport rate into brain was 20 percent below normal. This suggests that repressive changes of the glucose transport mechanism occur in brain endothelial cells in response to increased plasma glucose.*

Glucose is transported across the cerebral capillary endothelium by facilitated diffusion (*1*). It has been shown for other nutrients, for example, β-hydroxybutyrate, that the membrane constituent responsible for facilitated diffusion is subject to induction (*2*).

In 1959, Wyke (*3*) described a group of patients with "relative cerebral hypoglycemia" in whom symptoms indicative of hypoglycemia existed at normal plasma glucose concentrations. The condition of the patients improved upon elevation of the plasma glucose, suggesting insufficient capacity for glucose transport from blood to brain, compensated by the increased plasma glucose.

Diabetics with markedly elevated plasma glucose concentrations respond to rapid normalization of plasma glucose with symptoms of hypoglycemia, including hypothalamic excitation and increased sympathetic discharge, often referred to as "resetting of the glucostat" (*4*).

These clinical observations suggest an influence of chronically elevated plasma glucose concentrations on the transport capacity of the blood-brain barrier. The present study was undertaken to determine the influence of chronic hyperglycemia on the rate of glucose transfer from blood to brain. The study revealed a reduction of the maximum transport capacity that may be explained by mechanisms known from variation of gene expression (induction or repression).

Ninety-three rats were divided in two groups. The experimental group was rendered hyperglycemic by a single intraperitoneal injection of streptozotocin (50 mg per kilogram of body weight). The two groups were housed and handled in the same way for 3 weeks. Unidirectional blood-brain glucose transfer and blood and plasma flow rates of the parietal cortex were measured in both groups at different plasma glucose concentrations reached after administration of glucose or insulin.

Details of the glucose and insulin treatments and the determination of kinetic constants for glucose transport across the blood-brain barrier were given previously (*5*). The determination of kinetic constants was based on the equation

$$E^* = 1 - e^{-PS/F} \quad (1)$$

where E^* is the unidirectional extraction of labeled glucose, and

$$PS = \frac{T_{max}}{K_t + C_a} \quad (2)$$

and F is the plasma flow to brain. The notations T_{max} and K_t are used for the maximum reaction rate and the half-saturation constant of a transport process, respectively, and replace the symbols V_{max} and K_m commonly used for proper enzymatic reactions. C_a is the arterial plasma glucose concentration (*6*). We measured E^*, the fraction extracted in brain, by an integral method (*7*). According to this method

$$E^* = \frac{M^*(T)}{F \int_0^T C_a^*(t)\, dt} \quad (3)$$

in which $M^*(T)$ is the amount of labeled glucose in a sample of brain (excluding glucose in plasma), F the plasma flow rate into the sampled region, and $C_a^*(t)$ the arterial tracer glucose concentration. The integral was determined by withdrawal of arterial blood at a constant rate. The animals were decapitated 20

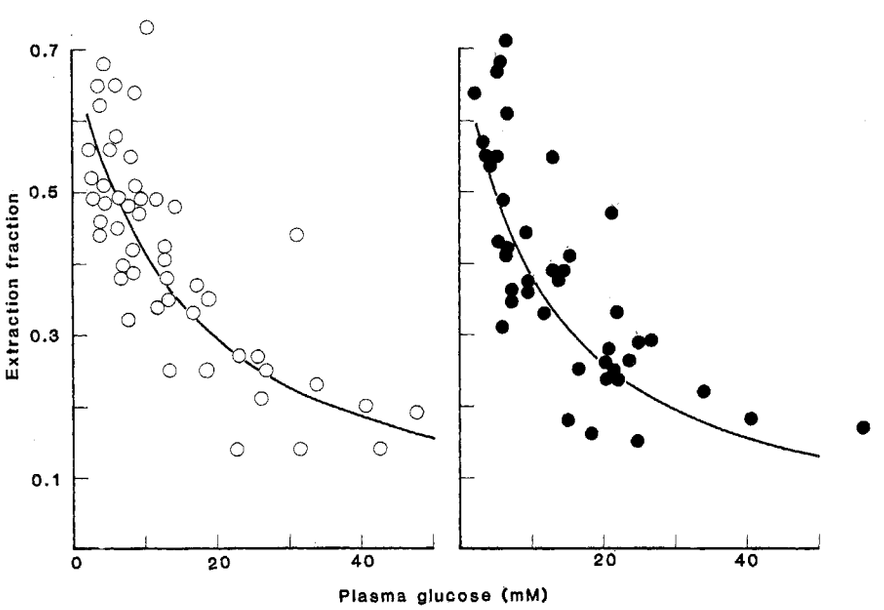

Fig. 1. Extraction of labeled glucose from the brains of control rats (○) and rats rendered hyperglycemic for 3 weeks by single intraperitoneal injection of streptozotocin (●). The extraction fractions were measured 20 seconds after a single intravenous injection of labeled glucose and labeled flow indicator (butanol), at the plasma glucose concentrations of arterial blood shown in the abscissa.

0036-8075/81/1023-0456$01.00/0